Supporting information for: Molecular Dynamics Investigation of the Influence of the Hydrogen Bond Networks in Ethanol/Water Mixtures on Dielectric Spectra

Javier Cardona,*,† Martin B. Sweatman,‡ and Leo Lue†

†*Department of Chemical and Process Engineering, University of Strathclyde, James Weir Building, 75 Montrose Street, Glasgow G1 1XJ, United Kingdom*

‡*School of Engineering, The University of Edinburgh, The King's Buildings, Sanderson Building, Mayfield Road, Edinburgh EH9 3JL, United Kingdom*

E-mail: j.cardona-amengual@strath.ac.uk

Phone: +44 (0)141 444 7321

Thermodynamic properties

Figure S1 shows the influence of composition on the density ρ, thermal expansion coefficient α_{p}, heat capacity $\mathrm{c_p}$, and isothermal compressibility κ_{T} of ethanol/water mixtures. In general, the main experimental trends are satisfactorily captured by the force fields employed in this work. The evolution of density (see Fig. S1a) is particularly well predicted, includ-

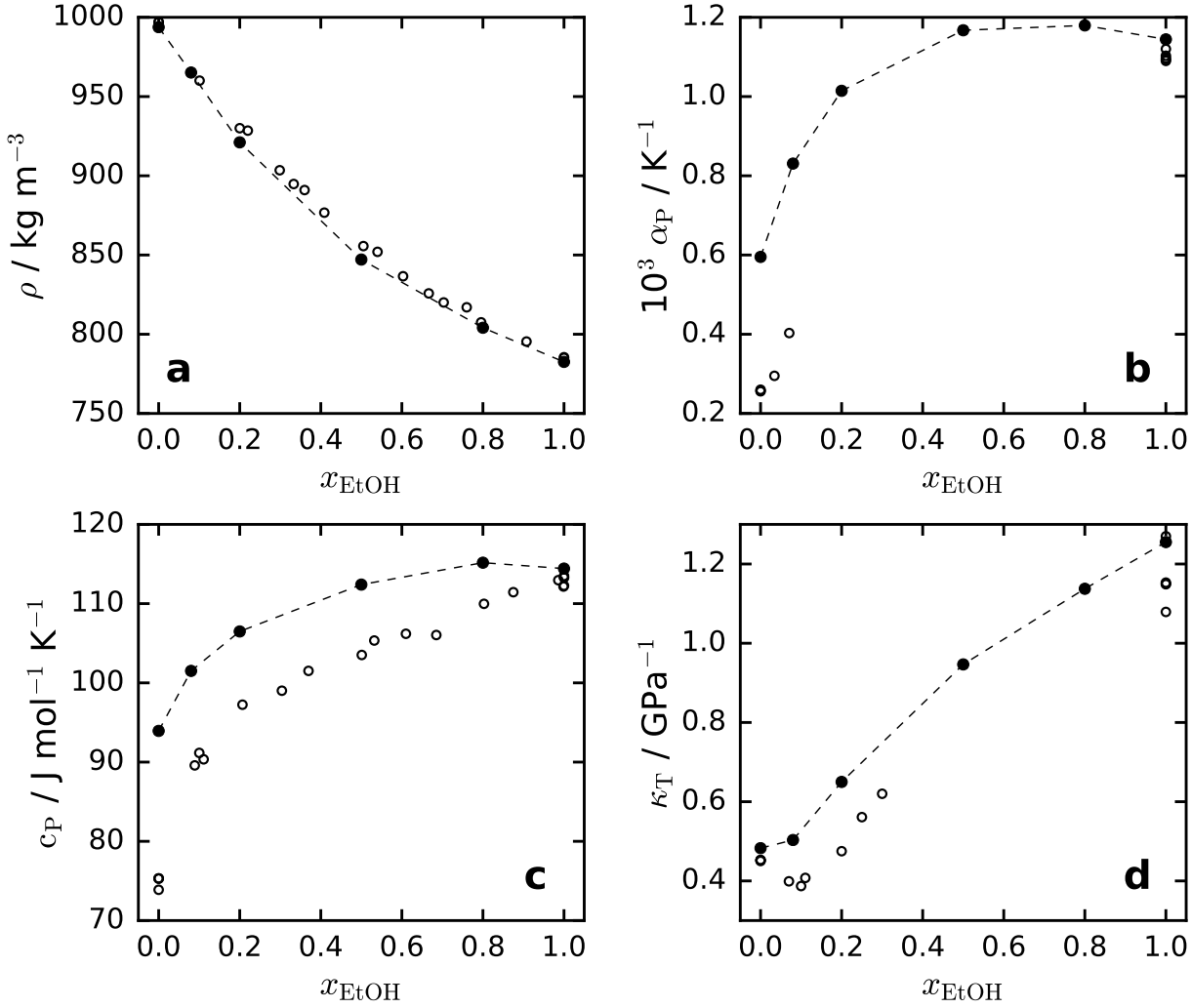

Figure S1: Influence of composition on a) density, b) thermal expansion coefficient, c) heat capacity and d) isothermal compressibility of ethanol/water mixtures at 298 K and 1 bar. Filled symbols represent results obtained from our simulations. Open symbols correspond to experimental data obtained from different sources: density ρ ,[S1,S2] thermal expansion coefficient α_{p},[S3–S11] heat capacity $\mathrm{c_p}$,[S12–S19] and isothermal compressibility κ_{T}.[S3,S9,S20–S28] Error bars are smaller than symbol sizes. The dashed lines are a guide to the eye.

ing a closer estimation of the density of pure water by the modified semi-flexible Fw-SPC model, with respect to the original fully flexible Fw-SPC model.[S29] The simulations provide excellent predictions for both the thermal expansion coefficient (see Fig. S1b) and heat capacity (see Fig. S1c) for pure ethanol, however, the results for pure water are somewhat overestimated. The restriction of bond stretching in the modified Fw-SPC model results in a higher thermal expansion coefficient and lower heat capacity than the original Fw-SPC model.[S29] The high values obtained for pure water explain the general overprediction of these properties with respect to experimental values at intermediate concentrations. Despite this, the variation with mixture concentration is preserved, especially for the heat capacity where more data are available for comparison. Finally, the isothermal compressibility clearly follows the experimental trend (see Fig. S1d), again with a slight overestimation with respect to the experimental data. The minimum of the isothermal compressibility observed in the experimental data at a $x_{\mathrm{EtOH}} \approx 0.1$ might be present in our simulation model; however, additional simulations in that concentration region would be required to confirm this feature. In general, the Fw-SPC presents slight deviations in the prediction of absolute values of some thermodynamic properties of water which affect the estimation of these properties of ethanol/water mixtures, particularly at low ethanol concentrations. However, this is compensated by a good prediction of dielectric properties, which is the main focus of this work.

The hydrogen bond network

Prior studies have shown how the dielectric response of alcohol/water mixtures is driven by the dynamics of their hydrogen bond network and the hydrophobic effects related to their alkyl groups. In line with the iceberg model suggested by Frank and Evans,[S30] the first hydration shell around hydrophobic groups has historically been assumed to have the structure of clathrate hydrates, in which water molecules are hydrogen-bonded in a configuration closer to a tetrahedral structure than bulk water itself. The more ordered structure would be characterized by a large entropy decrease and heat capacity rise with respect to bulk water. However, in recent years this assumption has been challenged by several experimental and theoretical studies,[S31–S38] which suggest the enhancement of hydrogen bonding in the first hydration shell of hydrophobic solutes does not actually occur, or at least not to a large enough extent to explain the significant entropy drop.[S39–S41] In these studies, this more ordered structure is associated to the formation of a cavity in the solvent in which the solute can be introduced.[S42] Although significant progress has been made in the study of the concentration dependence of the hydrogen bond network in alcohol/water mixtures, it is still not fully understood.

Using MD simulations with polarizable models, Noskov *et al.*[S43] have shown how hydrogen bonding is intensified in the first hydration shell surrounding hydrophobic groups but is more intensely depleted in the vicinity of hydroxyl groups, leading to a net depletion of hydrogen bonding in the first hydration shell of ethanol. This phenomenon is, however, balanced by a larger enhancement in the second hydration shell, which results in a global strengthening of the hydrogen bond network. At high ethanol concentrations, approximately above the equimolar mixture, a transition from a percolating network of hydrogen-bonded water molecules to a more disperse structure is clearly observed. The lower amount of water molecules in the second hydration shell diminishes its compensation effect, and the depletion of water hydrogen bonds in the first shell becomes dominant. As a consequence, the net outcome is a weakening of the global hydrogen bond structure. Zhong and Patel,[S44]

using a different polarizable model, agree with the net positive excess in water hydrogen bonding at low ethanol concentrations, although in their study they observed a depletion of hydrogen bonds in the surroundings of hydrophobic groups and an enhancement in the vicinity of hydroxyl groups in the first hydration shell, in contrast with Noskov's results. The contribution of the second hydration shell is also positive, but its magnitude is significantly smaller. More recently, Ghoufi *et al.*[S45] confirmed Noskov's observations for high ethanol concentrations using non-polarizable force fields. They explain the weakening of the hydrogen bond network as a transition from a percolating network formed by hydrogen-bonded water molecules to a non-percolating network in which water and ethanol form clusters of decreasing size as the concentration of ethanol increases. These clusters may, however, be the origin of the difficultly in separating water from ethanol at high concentrations. For concentrations higher than the azeotropic composition, water molecules were found to be fully dispersed, making their separation easier.

The experimental studies of Li *et al.*[S37] seem to agree with most of the previous conclusions and suggest a model with three critical alcohol compositions: $x_1 = 0.07$, $x_2 = 0.15$, and $x_3 = 0.60$. Below x_1, large hydration shells form around the hydrophobic groups of alcohol molecules. Above this concentration, extended hydrogen bond networks are generated as water molecules show a preference for the hydroxyl groups of the alcohols. The resulting hydrogen bond structure becomes increasingly stronger until a mole fraction x_2 is reached. At this point, a minimum in the diffusivity of alcohol molecules is observed, which corresponds to a situation in which the mixture achieves its most structured configuration. For higher concentrations, alcohol molecules tend to aggregate, reducing the strength of the hydrogen bond network, until reaching a point (x_3) in which water and ethanol diffusivities become independent.

In Fig. S2a, we show the effect of concentration on the size of the hydrogen bond network. In this work, a hydrogen bond is considered to exist when the distance between the hydrogen atom on the donor molecule and the oxygen atom on the acceptor molecule is less than 2.4 Å

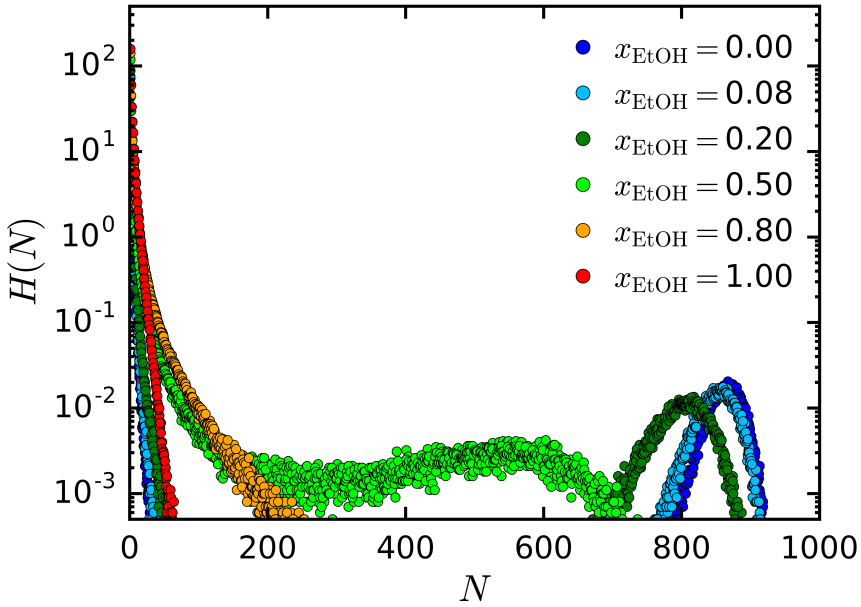

(a) All

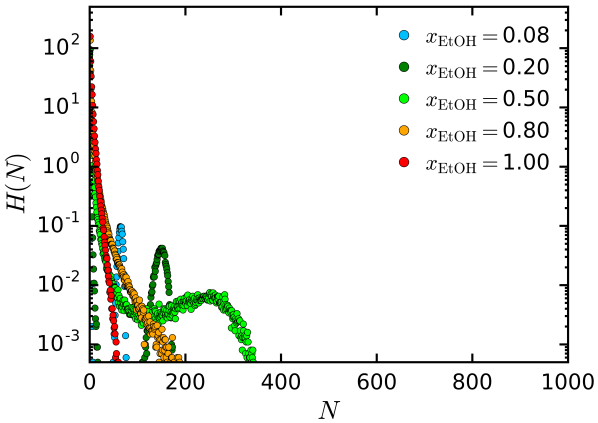

(b) Ethanol

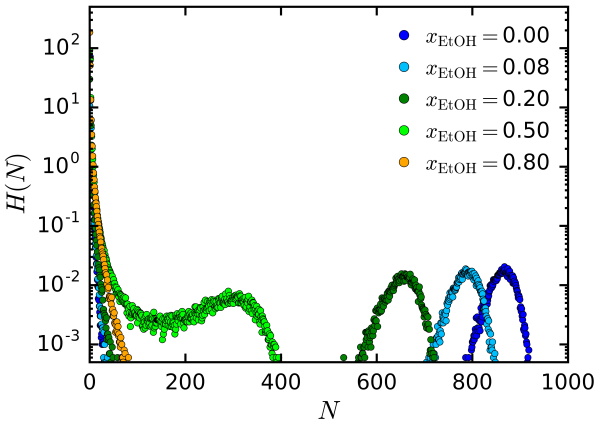

(c) Water

Figure S2: Effect of concentration on the cluster size distribution in ethanol/water mixtures at 298 K and 1 bar.

and the angle between the hydrogen bond and the covalent bond is greater than 150°.[S43] Figure S3 shows the change with concentration of the fraction of ethanol and water molecules that belong to extended networks (a network formed by more than half of the molecules in the mixture). The distributions of the number of molecules of each component of the mixture in these clusters are shown in Figs. S2b and S2c.

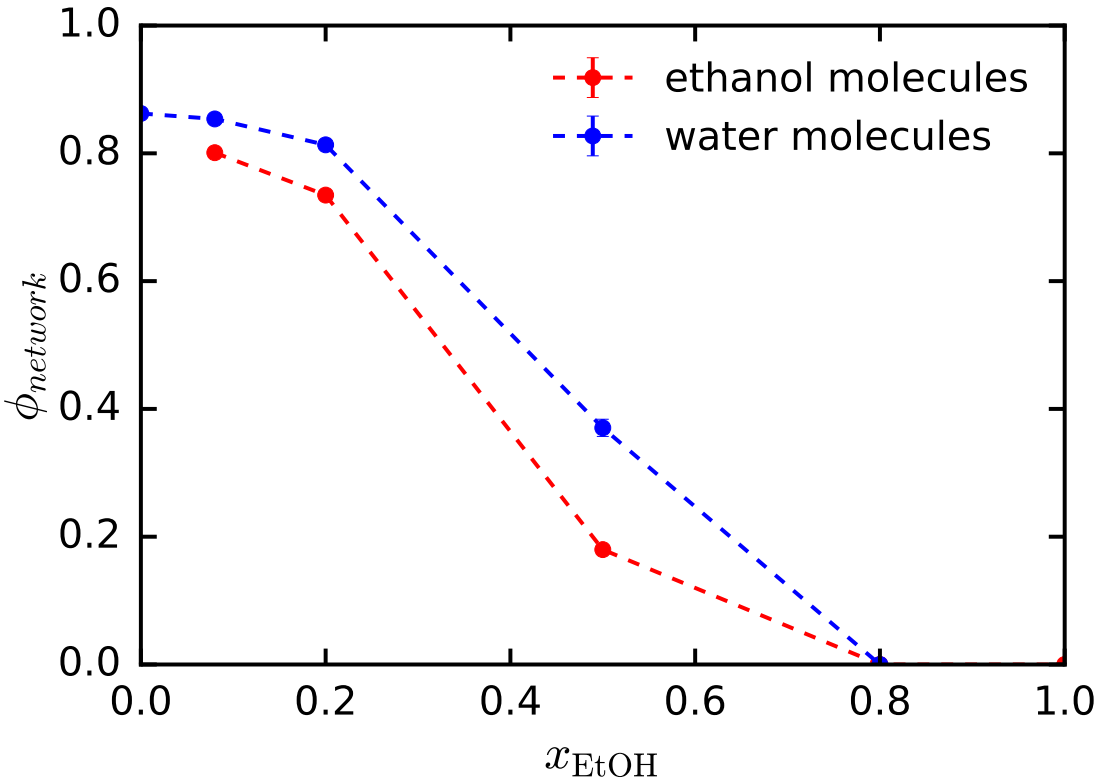

Figure S3: Effect of concentration on the fraction $\phi_{network}$ of molecules belonging to extended networks in ethanol/water mixtures at 298 K and 1 bar. An extended network is considered to be present when it is formed by more than half of the available molecules of each species. Error bars are smaller than the symbols size. Dashed lines are a guide to the eye.

Figure S4a shows the distribution of the number of hydrogen bonds formed by each molecule with any other molecule. The contributions of the number of hydrogen bonds formed by ethanol molecules with other ethanol molecules and with any molecule are presented in Figs. S4b and S4c, respectively. The distributions of the number of hydrogen bonds formed by water molecules with other water molecules and with any molecule are shown in Figs. S4d and S4e, respectively.

The results presented in Fig. S4 are used to obtain the evolution of the average number of hydrogen bonds with concentration shown in Fig. S5. As the concentration of ethanol in the mixture increases, the average number of hydrogen bonds formed by each molecule (black) decreases due to the lower availability of hydrogen bonding sites. Despite the disparity of

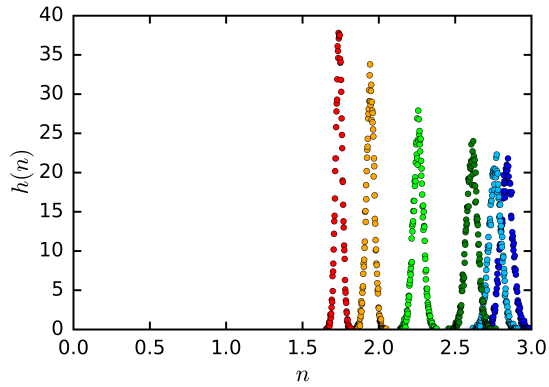

(a) All – All

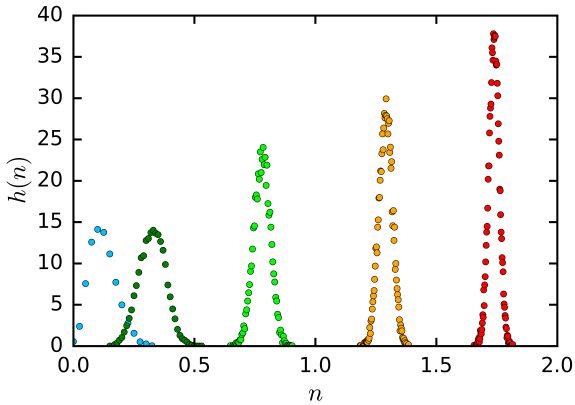

(b) Ethanol – Ethanol

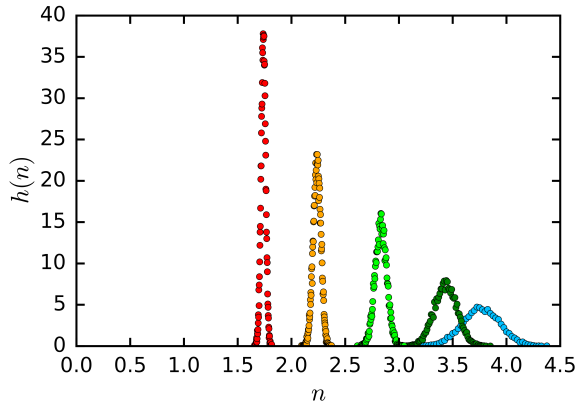

(c) Ethanol – All

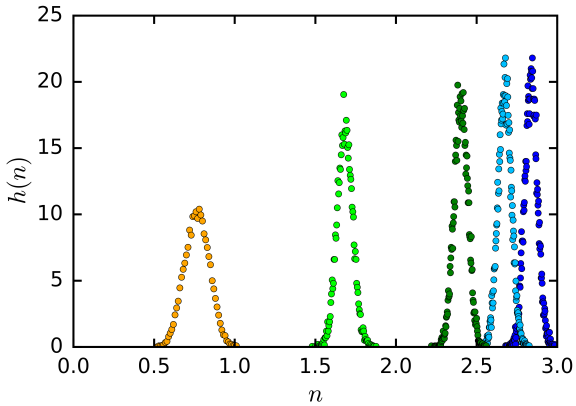

(d) Water – Water

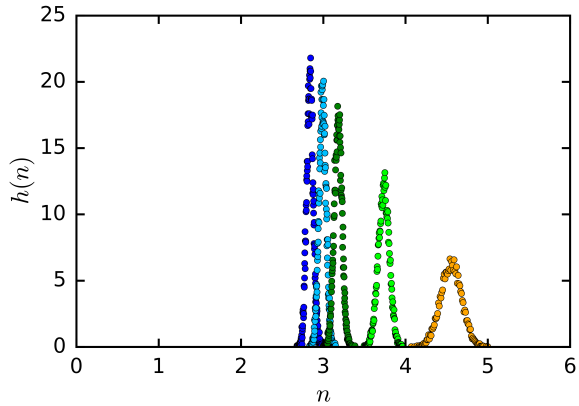

(e) Water – All

Figure S4: Effect of concentration on the distribution of the number of hydrogen bonds formed by each molecule in ethanol/water mixtures at 298 K and 1 bar.

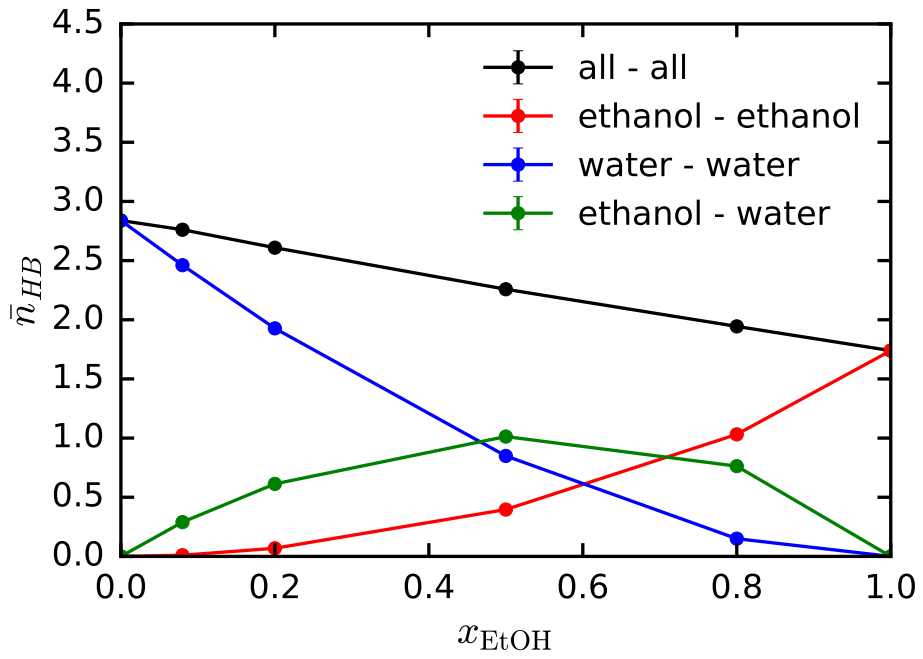

Figure S5: Effect of concentration on the average number of hydrogen bonds formed by each molecule ($\bar{n}_{HB}$) in ethanol/water mixtures at 298 K and 1 bar. Error bars are smaller than the symbols size. Solid lines are a guide to the eye.

approaches on how to define[S46] and count hydrogen bonds and the wide variety of results in the literature, the average number of hydrogen bonds obtained in this work falls within the range covered by previous studies for both ethanol[S38,S43] and water.[S47–S51] Figure S5 also shows the effect on the average number of hydrogen bonds between molecules of the same species (red and blue) and between molecules of different species (green). Initially, as the first ethanol molecules are added to pure water, they tend to associate with water molecules rather than with themselves. This is however not sufficient to counteract the depletion of water-water hydrogen bonds. As more ethanol molecules become available in the mixture, a preference towards forming hydrophobic clusters with themselves is clearly observed. Beyond the equimolar mixture, the percolating network formed by water-water and ethanol-water hydrogen bonds tends to vanish, and ethanol-ethanol clusters become predominant. These results agree with the main conclusions of an extensive study of the hydrogen bond network of ethanol/water mixtures recently carried out by Gereben and Pusztai.[S52]

References

(S1) Petong, P.; Pottel, R.; Kaatze, U. Water-Ethanol Mixtures at Different Compositions and Temperatures. A Dieletric Relaxation Study. *J. Phys. Chem. A* **2000**, *104*, 7420–7428.

(S2) Herráez, J.; Belda, R. Refractive Indices, Densities and Excess Molar Volumes of Monoalcohols + Water. *J. Solution Chem.* **2006**, *35*, 1315–1328.

(S3) Kell, G. S. Precise Representation of Volume Properties of Water at One Atmosphere. *J. Chem. Eng. Data* **1967**, *12*, 66–69.

(S4) Grant-Taylor, D. F.; Macdonald, D. D. Thermal Pressure and Energy-Volume Coefficients for the Acetonitrile + Water System. *Can. J. Chem.* **1976**, *54*, 2813–2819.

(S5) Hales, J.; Ellender, J. Liquid Densities from 293 to 490 K of Nine Aliphatic Alcohols. *J. Chem. Thermodyn.* **1976**, *8*, 1177–1184.

(S6) Dickinson, E.; Thrift, L. J.; Wilson, L. Thermal Expansion and Shear Viscosity Coefficients of Water + Ethanol + Sucrose Mixtures. *J. Chem. Eng. Data* **1980**, *25*, 234–236.

(S7) Costas, M.; Alonso, M. C.; Heintz, A. Experimental and Theoretical Study of the Apparent Molar Volumes of 1-Alcohols in Linear Hydrocarbons. *Berichte der Bunsengesellschaft fur physikalische Chemie* **1987**, *91*, 184–190.

(S8) Mier, W.; Oswald, G.; Tusel-Langer, E.; Lichtenthaler, R. Excess Enthalpy H^E of Binary Mixtures Containing Alkanes, Ethanol and Ethyl-Tert. Butyl Ether (ETBE). *Berichte der Bunsengesellschaft fur physikalische Chemie* **1995**, *99*, 1123–1130.

(S9) Marcus, Y. *The Properties of Solvents*; Wiley, 1998.

(S10) Orekhova, Z.; Ben-Hamo, M.; Manzurola, E.; Apelblat, A. Electrical Conductance and Volumetric Studies in Aqueous Solutions of Nicotinic Acid. *J. Solution Chem.* **2005**, *34*, 687–700.

(S11) Uosaki, Y.; Motoki, T.; Hamaguchi, T.; Moriyoshi, T. Excess Molar Volumes of Binary Mixtures of 1,3-dimethylimidazolidin-2-one with an Alkan-1-ol at the Temperatures 283.15 K, 298.15 K, and 313.15 K. *J. Chem. Thermodyn.* **2007**, *39*, 810–816.

(S12) Rivkin, S.; Winnikova, A. The Specific Heat of Aqueous Solutions of Ethyl Alcohol. *Chem. Ing. Tech.* **1965**, *37*, 556–560.

(S13) Vasilev, V.; Shevchenko, E.; Karapetyants, M.; Leonov, V.; Pavlova, V.; Krylova, T. Physico-chemical Properties of Copper Chloride Solutions in Mixed Ethanol - Water Solutions. *Izv. Vyssh. Uchebn. Zaved. Khim. Khim. Tekhnol.* **1978**, *21*, 1131–1138.

(S14) Vasilev, V.; Shevchenko, E.; Vorobev, A.; Vasileva, S. Heat Capacity and Density of the $CoCl_2$ - Ethanol - Water System at 298.15 K. *Izv. Vyssh. Uchebn. Zaved. Khim. Khim. Tekhnol.* **1985**, *28*, 52–55.

(S15) García-Miaja, G.; Troncoso, J.; Romaní, L. Density and Heat Capacity as a Function of Temperature for Binary Mixtures of 1-Butyl-3-methylpyridinium Tetrafluoroborate + Water, + Ethanol, and + Nitromethane. *J. Chem. Eng. Data* **2007**, *52*, 2261–2265.

(S16) Rubini, K.; Francesconi, R.; Bigi, A.; Comelli, F. Excess Molar Enthalpies and Heat Capacities of Dimethyl Sulfoxide + Seven Normal Alkanols at 303.15 K and Atmospheric Pressure. *Thermochim. Acta* **2007**, *452*, 124–127.

(S17) Anouti, M.; Caillon-Caravanier, M.; Dridi, Y.; Jacquemin, J.; Hardacre, C.; Lemordant, D. Liquid Densities, Heat Capacities, Refractive Index and Excess Quantities for Protic Ionic Liquids + Water Binary System. *J. Chem. Thermodyn.* **2009**, *41*, 799–808.

(S18) Nie, N.; Zheng, D.; Dong, L.; Li, Y. Thermodynamic Properties of the Water + 1-(2-Hydroxylethyl)-3-methylimidazolium Chloride System. *J. Chem. Eng. Data* **2012**, *57*, 3598–3603.

(S19) Hou, Y.; Sha, Z.; Wang, Y. Determination of Specific Heat Capacity of Butylated Hydroxytoluene - Ethanol Binary System by DSC Method. *Shiyou Huagong* **2012**, *41*, 215–218.

(S20) Jung, K. MSc Thesis. M.Sc. thesis, University of Calgary, 1969.

(S21) Sahli, B. P.; Gager, H.; Richard, A. J. Ultracentrifugal Studies of the Isothermal Compressibilities of Organic Alcohols and Alkanes. Correlation with Surface Tension. *J. Chem. Thermodyn.* **1976**, *8*, 179–188.

(S22) Moriyoshi, T.; Inubushi, H. Compressions of Some Alcohols and Their Aqueous Binary Mixtures at 298.15 K and at Pressures up to 1400 atm. *J. Chem. Thermodyn.* **1977**, *9*, 587–592.

(S23) Diaz Peña, M.; Tardajos, G. Isothermal Compressibilities of n-1-alcohols from Methanol to 1-dodecanol at 298.15, 308.15, 318.15, and 333.15 K. *J. Chem. Thermodyn.* **1979**, *11*, 441–445.

(S24) Brostow, W.; Grindley, T.; Macip, M. Volumetric Properties of Organic Liquids as a Function of Temperature and Pressure: Experimental Data and Prediction of Compressibility. *Mater. Chem. Phys.* **1985**, *12*, 37–97.

(S25) Hamad, E.; Mansoori, G.; Matteoli, E.; Lepori, L. Relations Among Concentration Fluctuation Integrals in Mixtures (Theory and Experiments). *Z. Phys. Chem.* **1989**, *162*, 27–45.

(S26) Vedamuthu, M.; Singh, S.; Robinson, G. W. Properties of Liquid Water. 4. The

Isothermal Compressibility Minimum near 50°C. *J. Phys. Chem.* **1995**, *99*, 9263–9267.

(S27) Papaioannou, D.; Panayiotou, C. Viscosity of Binary Mixtures of Propylamine with Alkanols at Moderately High Pressures. *J. Chem. Eng. Data* **1995**, *40*, 202–209.

(S28) Doi, H.; Tamura, K.; Murakami, S. Thermodynamic Properties of Aqueous Solution of 2-isobutoxyethanol at T = (293.15, 298.15, and 303.15) K, Below and Above LCST. *J. Chem. Thermodyn.* **2000**, *32*, 729–741.

(S29) Cardona, J.; Fartaria, R.; Sweatman, M. B.; Lue, L. Molecular Dynamics Simulations for the Prediction of the Dielectric Spectra of Alcohols, Glycols and Monoethanolamine. *Mol. Simul.* **2016**, *42*, 370–390.

(S30) Frank, H. S.; Evans, M. W. Free Volume and Entropy in Condensed Systems III. Entropy in Binary Liquid Mixtures; Partial Molal Entropy in Dilute Solutions; Structure and Thermodynamics in Aqueous Electrolytes. *J. Chem. Phys.* **1945**, *13*, 507–532.

(S31) Dixit, S.; Soper, A. K.; Finney, J. L.; Crain, J. Water Structure and Solute Association in Dilute Aqueous Methanol. *Europhys. Lett.* **2002**, *59*, 377–383.

(S32) Raschke, T. M.; Levitt, M. Nonpolar Solutes Enhance Water Structure Within Hydration Shells while Reducing Interactions between Them. *Proc. Natl. Acad. Sci. U. S. A.* **2005**, *102*, 6777–6782.

(S33) Laage, D.; Stirnemann, G.; Hynes, J. T. Why Water Reorientation Slows without Iceberg Formation around Hydrophobic Solutes. *J. Phys. Chem. B* **2009**, *113*, 2428–2435.

(S34) Petersen, C.; Tielrooij, K.; Bakker, H. J. Strong Temperature Dependence of Water Reorientation in Hydrophobic Hydration Shells. *J. Chem. Phys.* **2009**, *130*, 214511.

(S35) Garde, S.; Patel, A. J. Unraveling the Hydrophobic Effect, One Molecule at a Time. *Proc. Natl. Acad. Sci. U. S. A.* **2011**, *108*, 16491–16492.

(S36) Guevara-Carrion, G.; Vrabec, J.; Hasse, H. Prediction of Self-diffusion Coefficient and Shear viscosity of Water and its Binary Mixtures with Methanol and Ethanol by Molecular Simulation. *J. Chem. Phys.* **2011**, *134*, 074508.

(S37) Li, R.; D'Agostino, C.; McGregor, J.; Mantle, M. D.; Zeitler, J. A.; Gladden, L. F. Mesoscopic Structuring and Dynamics of Alcohol/Water Solutions Probed by Terahertz Time-Domain Spectroscopy and Pulsed Field Gradient Nuclear Magnetic Resonance. *J. Phys. Chem. B* **2014**, *118*, 10156–10166.

(S38) Gereben, O.; Pusztai, L. Investigation of the Structure of Ethanol-Water Mixtures by Molecular Dynamics Simulation I: Analyses Concerning the Hydrogen-Bonded Pairs. *J. Phys. Chem. B* **2015**, *119*, 3070–3084.

(S39) Galamba, N. Water's Structure around Hydrophobic Solutes and the Iceberg Model. *J. Phys. Chem. B* **2013**, *117*, 2153–2159.

(S40) Graziano, G. Comment on 'Water's Structure around Hydrophobic Solutes and the Iceberg Model'. *J. Phys. Chem. B* **2014**, *118*, 2598–2599.

(S41) Galamba, N. Reply to 'Comment on 'Water's Structure around Hydrophobic Solutes and the Iceberg Model". *J. Phys. Chem. B* **2014**, *118*, 2600–2603.

(S42) Davis, J. G.; Gierszal, K. P.; Wang, P.; Ben-Amotz, D. Water Structural Transformation at Molecular Hydrophobic Interfaces. *Nature* **2012**, *491*, 582–585.

(S43) Noskov, S. Y.; Lamoureux, G.; Roux, B. Molecular Dynamics Study of Hydration in Ethanol-Water Mixtures Using a Polarizable Force Field. *J. Phys. Chem. B* **2005**, *109*, 6705–6713.

(S44) Zhong, Y.; Patel, S. Electrostatic Polarization Effects and Hydrophobic Hydration in Ethanol-Water Solutions from Molecular Dynamics Simulations. *J. Phys. Chem. B* **2009**, *113*, 767–778.

(S45) Ghoufi, A.; Artzner, F.; Malfreyt, P. Physical Properties and Hydrogen-Bonding Network of Water-Ethanol Mixtures from Molecular Dynamics Simulations. *J. Phys. Chem. B* **2016**, *120*, 793–802.

(S46) Gereben, O.; Pusztai, L. Hydrogen Bond Connectivities in Water-Ethanol Mixtures: On the Influence of the H-Bond Definition. *J. Mol. Liq.* **2016**, *220*, 836–841.

(S47) Nieto-Draghi, C.; Avalos, J. B.; Rousseau, B. Dynamic and Structural Behavior of Different Rigid Nonpolarizable Models of Water. *J. Chem. Phys.* **2003**, *118*, 7954–7964.

(S48) Wernet, P.; Nordlund, D.; Bergmann, U.; Cavalleri, M.; Odelius, M.; Ogasawara, H.; Näslund, L. Å.; Hirsch, T. K.; Ojamäe, L.; Glatzel, P.; Pettersson, L. G. M.; Nilsson, A. The Structure of the First Coordination Shell in Liquid Water. *Science* **2004**, *304*, 995–999.

(S49) Smith, J. D.; Cappa, C. D.; Wilson, K. R.; Messer, B. M.; Cohen, R. C.; Saykally, R. J. Energetics of Hydrogen Bond Network Rearrangements in Liquid Water. *Science* **2004**, *306*, 851–853.

(S50) He, C.; Lian, J.; Jiang, Q. Electronic Structures and Hydrogen Bond Network of Ambient Water and Amorphous Ices. *Chem. Phys. Lett.* **2007**, *437*, 45–49.

(S51) Rastogi, A.; Ghosh, A. K.; Suresh, S. In *Thermodynamics - Physical Chemistry of Aqueous Systems, Hydrogen Bond Interactions Between Water Molecules in Bulk Liquid, Near Electrode Surfaces and Around Ions*; Moreno-Pirajan, J. C., Ed.; InTech, 2011; Chapter 13.

(S52) Gereben, O.; Pusztai, L. Cluster Formation and Percolation in Ethanol-Water Mixtures. *Chem. Phys.* **2017**, *496*, 1–8.